Journal of Biomolecular NMR, 2 (1992) 361–372
ESCOM

J-Bio NMR 066

Spatial structure of (34–65)bacterioopsin polypeptide in SDS micelles determined from nuclear magnetic resonance data

Andrew L. Lomize, Konstantine V. Pervushin and Alexander S. Arseniev*

M.M. Shemyakin Institute of Bioorganic Chemistry, Russian Academy of Sciences, Ul. Miklukho-Maklaya 16/10, Moscow, V-437, Russia

Received 13 November 1991
Accepted 3 April 1992

Keywords: Bacteriorhodopsin; α-Helix; Micelles; ^{1}H NMR; Distance geometry

SUMMARY

The spatial structure of a synthetic 32-residue polypeptide, an analog of the membrane-spanning segment B (residues 34–65) of bacterioopsin of *Halobacterium halobium*, incorporated into perdeuterated sodium dodecyl sulfate micelles, was determined from ^{1}H NMR data. The structure determination included the following steps: (1) local structure analysis; (2) structure calculations using the distance geometry program DIANA; (3) systematic search for energetically allowed side-chain rotamers consistent with NOESY cross-peak volumes; (4) random generation of peptide conformations in allowed conformational space. The obtained structure has a right-handed α-helical region from Lys^{41} to Leu^{62} with a kink of 27° at Pro^{50}. The C-cap Gly^{63} adopts a conformation with $\varphi = 87 \pm 6$, $\psi = 43 \pm 10$° typical to a left-handed helix. The N-terminal part (residues 34–40) is exposed to the aqueous phase and lacks an ordered conformation. The secondary structure of segment B in micelles is consistent with the high-resolution electron cryomicroscopy model of bacteriorhodopsin (Henderson et al. (1990) *J. Mol. Biol.*, **213**, 899–929).

INTRODUCTION

Bacteriorhodopsin (BR) is a protein of the purple membrane of *Halobacterium halobium* (see Ovchinnikov, 1982; Dencher, 1983; Stoeckenius, 1985 for review). BR has one polypeptide chain of 248 amino acid residues arranged as 7 α-helical membrane-spanning segments A–G, which surround the retinal chromophore bound via a Schiff base to Lys^{216} (Bayley et al., 1981). The 3D model of BR has been derived from low-resolution electron cryomicroscopy (ECM) data for the purple membrane (about 3 and 10 Å in parallel and normal to the membrane surface planes) (Henderson et al., 1990).

Previously (Arseniev et al., 1987) an approach to the spatial structure reconstruction of BR

* To whom correspondence should be addressed.

based on the NMR data was proposed. This approach consists in (1) determination of the spatial structure of isolated fragments of BR in organic milieu or micelles using NMR techniques and (2) docking of these fragments using NMR and other data on contacts between fragments. Following this approach we have determined the secondary structure of synthetic (Arseniev et al., 1988; Maslennikov et al., 1990,1991a) and proteolytic bacterioopsin fragments (Barsukov et al., 1990; Abdulaeva et al., 1991).

The 34–65 segment of bacterioopsin (sB) in chloroform–methanol (1:1) solution forms a right-handed α-helix 37–64, which is most stable in the 42–60 region (Maslennikov et al., 1991b). These data agree with the 38–62 α-helix in the ECM model of BR (Henderson et al., 1990). To verify the environmental influence on the spatial structure of BR fragments, we analyzed the structure of sB incorporated into sodium dodecyl-d_{25} sulfate (SDS-d_{25}) micelles mimicking the bilayer membrane. The sequential ^{1}H NMR assignment of sB in SDS-d_{25} micelles has been described (Pervushin et al., 1991). The present paper deals with the spatial structure calculation of sB.

MATERIALS AND METHODS

NMR measurements

The NMR sample preparation, detection and assignment of ^{1}H NMR spectra of sB incorporated into SDS-d_{25} micelles were described previously (Pervushin et al., 1991). Volumes of 358 cross peaks were measured in the NOESY spectrum recorded at 600 MHz (Varian 'UNITY 600') with $\tau_m = 200$ ms.

Nonselective spin-lattice relaxation times (T_1) of sB protons were measured by the inversion-recovery technique. Since the error in T_1 values has a small effect on calculated NOESY cross-peak volumes (Sobol and Arseniev, 1988), we used mean T_1 values for the groups of protons (0.92 s for NH protons, 0.9 s for α-protons, 0.7 s for β-, γ-, and δ-protons, 1.6 s for aromatic protons).

Most of the cross peaks in phase-sensitive DQF-COSY spectra were not suitable for measuring the proton spin-spin coupling constants of H-NC^{α}-H and H-$C^{\alpha}C^{\beta}$-H fragments since the line widths of resonances (12–16 Hz) are larger than the constants. For 5 residues located in the 48, 54, 56, 58 and 60 positions the $C^{\alpha}H/C^{\beta 2}H$ and $C^{\alpha}H/C^{\beta 3}H$ cross peaks appear with essentially different amplitude in DQF-COSY spectra. For these residues χ^1 angles were restrained to exclude the *gauche* orientation of both β-protons relative to the α-proton.

Theoretical evaluation of NOESY cross-peak volumes

The matrix of NOESY cross-peak volumes $\mathbb{V}(\tau_m)$ was evaluated as (Bodenhausen and Ernst, 1982; Bremer et al., 1984; Keepers and James, 1984):

$$\mathbb{V}(\tau_m) = \exp[-\mathbb{R}\tau_m]\mathbb{V}_0 = \mathbb{D}\exp[-\mathbb{L}\tau_m]\mathbb{D}^{-1}\mathbb{V}_0 \quad (1)$$

where τ_m is mixing time, $\mathbb{R}$ is relaxation matrix, $\mathbb{D}$ is matrix of eigenvectors of $\mathbb{R}$, $\mathbb{L}$ is diagonal matrix of eigenvalues of $\mathbb{R}$ and $\mathbb{V}_0$ is diagonal matrix describing the steady state of the spin system at the beginning of the NOESY pulse sequence.

Relaxation matrix $\mathbb{R}$ elements σ_{pq} were calculated from proton coordinates, effective rotational correlation time τ_c of the molecule and nonselective spin-lattice relaxation times T_1 of protons (Sobol and Arseniev, 1988). To calculate cross-relaxation rates of methyl protons, the model of

rapid jumps between 3 discrete states in the isotropically rotating molecule (Tropp, 1980) was used.

To consider an unequilibrium steady state of the spin system, the elements of the diagonal matrix $\mathbb{V}_0$ were evaluated as (Sobol and Arseniev, 1988):

$$v_{pp}^0 = 1 - \exp[(t_2 + d_1)/T_{1p}] \tag{2}$$

where t_2 and d_1 are acquisition time and relaxation delay of the NOESY pulse sequence and T_{1p} is the experimentally measured mean time of nonselective spin-lattice relaxation of a given proton p.

NMR-derived upper distance constraints

The set of 238 upper distance limits $\{d_k\}$ was derived from volumes of 358 cross peaks measured in NOESY spectra. These limits were adjusted to normalized cross-peak volumes $\{\bar{V}^{obs}\}$ as follows:

$$d_k = \begin{cases} A[\bar{V}_k^{exp} - \bar{V}_0]^{-1/6}, & \text{if } \bar{V}_k^{exp} > \bar{V}_0 \\ R, & \text{if } \bar{V}_k^{exp} \le \bar{V}_0 \end{cases} \tag{3}$$

$$\bar{V}_k^{exp} = V_k^{exp}/(1/N \sum_{j=1}^{N} V_j^{exp}),$$

where N is the number of measured cross-peak volumes. Parameters A = 272.0 and $\bar{V}_0 = 0.18$ in Eq. 3 were obtained from the maximum volumes $\{\bar{V}_k^{exp}\}$ of cross peaks C^zH_i/NH_i and C^zH_i/HN_{i+1} measured in NOESY spectra and characteristic distances of 2.7 and 3.6 Å in right-handed helices. The parameter R = 5 Å is the upper limit for the low-volume NOESY cross peaks with $\bar{V}_k^{exp} \le \bar{V}_0$. Since the spin-diffusion effect was neglected, some upper limits were underestimated. The spin diffusion might affect mainly the constraints of side-chain geminal protons treated by DIANA as pseudoatoms. A summary of the sequential upper distance constraints used in the distance geometry calculation of sB is shown in Fig. 1a. Also 36 distance restraints were used to define 18 hydrogen bonds within the α-helical region (residues 42–63) that were identified previously based on both NOE and amide-exchange data (Pervushin et al., 1991). Preliminary structure calculations without inclusion of the hydrogen-bond restraints had shown the predicted hydrogen bonds to be quite compatible with the experimentally derived distance constraints.

Correspondence of calculated sB conformations to experimental NOESY data

To evaluate the correspondence of calculated sB conformations to NOESY spectra, the penalty functions F_v and F_r (Lomize et al., 1990) were constructed. The F_v function compares the theoretical (V^{the}) and experimental (V^{exp}) NOESY cross-peak volumes:

$$F_v = 1/N \sum_{k=1}^{N} \begin{cases} |\bar{V}_k^{exp} - \bar{V}_k^{the}| - \Delta V_k, & \text{if } |\bar{V}_k^{exp} - \bar{V}_k^{the}| > \Delta V_k \\ 0, & \text{if } |\bar{V}_k^{exp} - \bar{V}_k^{the}| \le \Delta V_k \end{cases} \tag{4}$$

$$\bar{V}_k = V_k/(1/N \sum_{j=1}^{N} V_j)$$

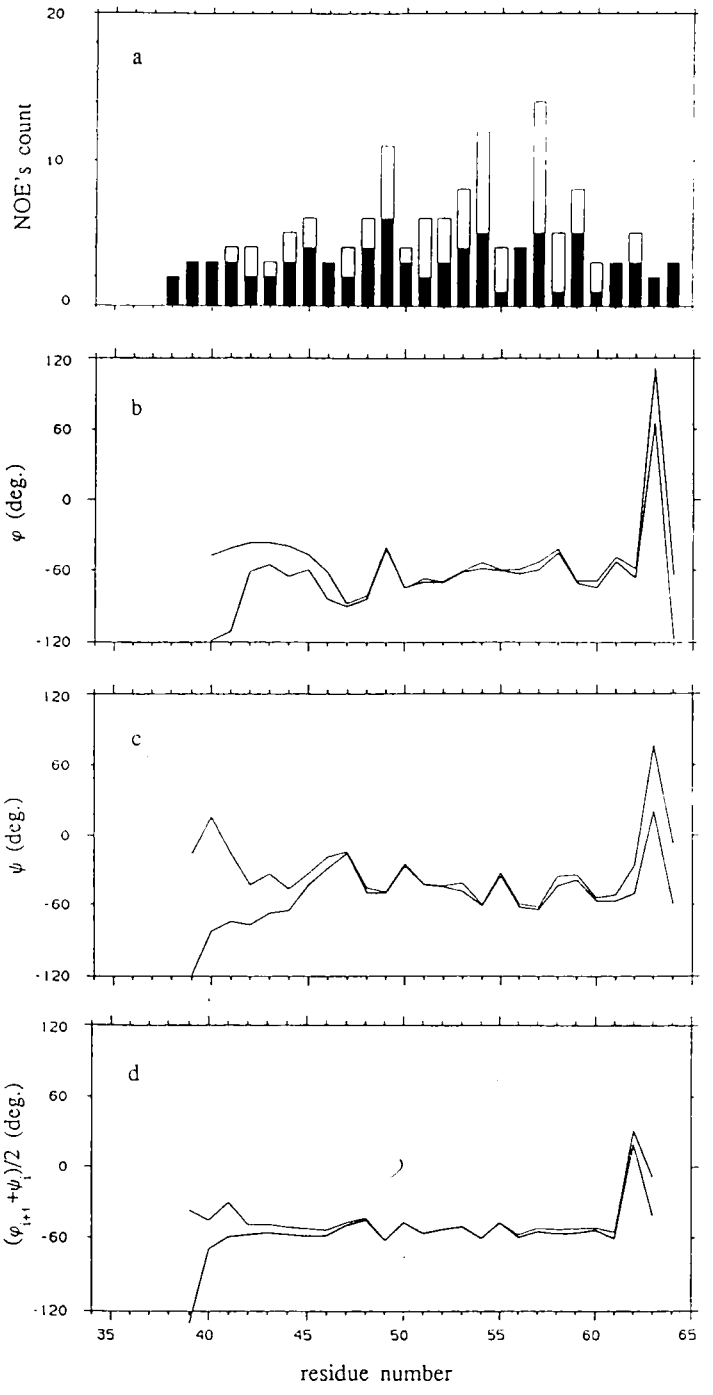

Fig. 1. Variations of φ, ψ and $(\varphi_{i+1}+\psi_i)/2$ angles (b,c,d) throughout the 20 best DIANA conformations vs. the amino acid sequence of sB. For comparison the number of sequential (i to $i+1$) and longer range (greater than i to $i+1$) distance restraints per residue are shown by filled and open rectangles, respectively (a).

where N is the number of NOESY cross peaks to be compared and $\bar{V}_k^{exp}$, $\bar{V}_k^{the}$ are normalized cross-peak volumes, ΔV_k is an error of the V_k^{exp} volume estimated as follows:

$$\Delta V_k = \max \{\Delta V_1, \Delta V_2 * \bar{V}_k^{exp}\}, \tag{5}$$

where ΔV_1 is the absolute error corresponding to the noise level in the NOESY spectrum and ΔV_2 is the relative error of measuring the V_k^{exp} volume. For the NOESY spectra of sB, ΔV_1 and ΔV_2 were estimated as 0.1 and 0.2, respectively.

The F_r function compares the interproton distances $\{r_k\}$ in the obtained conformation with those calculated based on NOESY cross-peak volumes:

$$F_r = [1/N \sum_{k=1}^{N} (\Delta r_k)^2]^{1/2} \tag{6}$$

where Δr_k is an interproton distance mismatch:

$$\Delta r_k = \begin{cases} 0, & \text{if } r_k^+ \geq r_k \geq r_k^- \\ r_k - r_k^+, & \text{if } r_k > r_k^+ \\ r_k - r_k^-, & \text{if } r_k < r_k^- \end{cases} \tag{7}$$

The interval of distances $[r_k^-, r_k^+]$ corresponding to the experimental volume V_k^{exp} was evaluated by the '$1/r^6$' law:

$$r_k^{\pm} = r_k [\bar{V}_k^{the} / (\bar{V}_k^{exp} \pm \Delta V_k)]^{1/6} \tag{8}$$

For overlapped cross peaks with a contribution of N pairs of p and q protons, the $\bar{V}_k^{the}$ value is the sum of the corresponding V_{pq} elements of the $\mathbb{V}(\tau_m)$ matrix and r_k is an effective distance instead of individual interproton distances r_{pq}:

$$r_k = \left(\sum_{p,q}^{N} r_{pq}^{-6} \right)^{-1/6} \tag{9}$$

The F_v and F_r functions depend on the stereospecific assignment of protons at prochiral centers. These functions were evaluated with all possible variants of the stereospecific assignments. Eventually the variant with minimum penalty functions was accepted.

RESULTS AND DISCUSSION

Computation of spatial structure of sB in SDS micelles

The reconstruction of the sB spatial structure was performed in 4 steps: (1) local structure analysis with the program CONFORNMR (Lomize et al., 1990) to obtain restraints for φ, ψ, χ^1 and χ^2 torsion angles, stereospecific assignments of protons at prochiral centers and to estimate the rotational correlation time τ_c of the molecule, (2) distance geometry calculations using the pro-

gram DIANA (Güntert et al., 1991), (3) energy refinement and systematic search for energetically allowed side-chain rotamers consistent with NOESY cross-peak volumes using the program CONFORNMR, (4) random generation and analysis of peptide conformations with allowed side-chain rotamers. The ECEPP/2 force field (Momany et al., 1975; Nemethy et al., 1983) was used.

The lack of sufficient NMR information about the N-terminal 34–38 residues prevents us from modelling its conformation. Therefore, the structure calculations were undertaken on a truncated molecule including residues 39–65.

(1) The local structure analysis

The local structure of sB was analyzed using the $F_r(\varphi_i,\psi_i,\chi_i^1,\tau_c)$ dependencies (see Eqs. 6–9) for each dipeptide unit i of the polypeptide including all protons of residue i and the amide proton of residue $i+1$.

The correlation time τ_c was determined as a minimum of $F_r^{min}(\tau_c)$ dependence for each dipeptide unit, where $F_r^{min}(\tau_c)$ is the global minimum value of $F_r(\varphi_i,\psi_i,\chi_i^1)$ at a given τ_c. For 12 dipeptide units the minima of $F_r(\tau_c)$ dependencies were within 2–6 ns. The other dipeptide units have no well-defined minima due to an insufficient number of experimental NOESY cross-peak volumes. This analysis led to the τ_c value of 4 ns used in further calculations.

TABLE I

χ^1 TORSION ANGLES (DEGREE ± STANDARD DEVIATION) FOUND IN 20 DIANA CONFORMATIONS (DIANA) AND IN 20 FINAL CONFORMATIONS AFTER EXHAUSTIVE SEARCH AND ENERGY MINIMIZATION (SEARCH)

Residue	DIANA	SEARCH
Lys^{40}	−78 ± 9	−171 ± 8, −74 ± 5
Lys^{41}	−115 ± 32	−167 ± 6, −76 ± 8
Phe^{42}	167 ± 3	175 ± 1
Tyr^{43}	172 ± 19, −80 ± 4	176 ± 1
Ile^{45}	−59 ± 10	−81 ± 1
Thr^{46}	52 ± 30, −109 ± 37	28 ± 4
Thr^{47}	60 ± 13, −45 ± 36	41 ± 2
Leu^{48}	−88 ± 3	173 ± 6
Val^{49}	−144 ± 5	163 ± 2
Ile^{52}	−97 ± 1	−75 ± 9
Phe^{54}	−167 ± 13, −105 ± 8	−180 ± 5
Thr^{55}	−28 ± 14	−62 ± 2
Nle^{56}	−96 ± 2	−162 ± 12, −81 ± 6
Tyr^{57}	−151 ± 5	174 ± 1
Leu^{58}	−73 ± 6	−168 ± 12, −68 ± 2
Ser^{59}	51 ± 31, −87 ± 9, 158 ± 8	58 ± 15, −61 ± 4
Nle^{60}	−75 ± 8	−166 ± 11, −74 ± 13
Leu^{61}	−159 ± 9	−177 ± 4
Leu^{62}	−165 ± 16, −78 ± 7	−158 ± 14, −75 ± 12
Tyr^{64}	−90 ± 5	−82 ± 10

To figure out the restraints for the φ and ψ torsion angles, we built $F_r(\varphi_i,\psi_i)$ maps for each χ_i^1, χ_i^2 side-chain rotamer and outlined φ_i–ψ_i regions with $F_r - F_r^{min} \leq 0.2$ Å; χ_i^1, χ_i^2 angles were kept at -60 ± 30, 60 ± 30 and $180 \pm 30°$. φ and ψ torsion angles were constrained to an interception between these (φ-ψ)-regions with sterically allowed ones. In this way we obtained 58 restraints for φ, ψ and χ^1 angles. For all residues the constrained (φ-ψ)-regions agree with the previously proposed α-helix Lys^{41} to Tyr^{62} of sB (Pervushin et al., 1991).

(2) Distance geometry calculations with the program DIANA

Structures were calculated with the program DIANA (Güntert et al., 1991) by optimizing randomly generated starting conformations according to the standard protocol. It includes minimization at 6 levels 0, 1, 2, 3, 4, 5 with weighting factors for experimental upper and lower distance limits set to 1, for van der Waals' lower distance limits 0.2 and for torsion angle restraints 20°.

A set of the 20 best DIANA conformations with final target functions less than 3.5, sum of residual violations of upper distance limits < 11 Å, steric repulsion < 2 Å and torsion angle constraints < 13 $Å^2$ was obtained. The maximum values of individual violations of these kinds were less than 0.8 Å, 0.3 Å, and 7 $Å^2$, respectively. The root-mean-square deviation (RMSD) of coordinates of the 20 DIANA conformations was 0.51 ± 0.17 Å for backbone atoms and 1.37 ± 0.25 Å for all heavy atoms of the residues 39–65.

Figures 1b and c show the variations of the backbone torsion angles φ and ψ. Residues 42–62 are in α-helical conformation (RMSD of coordinates of 20 conformations was 0.19 ± 0.06 Å for backbone atoms and 1.05 ± 0.25 Å for all heavy atoms). The smallest variation of φ and ψ angles is observed in the 47–62 region, increasing toward the N- and C-termini. The helical conformation of the peptide was preserved in the 42–62 region, since the parameter $(\varphi_{i+1} + \psi_i)/2$ (Fig. 1d) remained conservative. Large variations in φ and ψ angles in the N-terminal were caused by the variability of peptide group orientations at the 42–46 region of the α-helix where amide NH protons did not participate in hydrogen bonds. C-cap Gly^{63} ($\varphi = 87 \pm 6°$, $\psi = 43 \pm 10°$) adopts a conformation corresponding to the left-handed helix. This conformation is fixed by 12 medium-range NOE contacts stemming from $C^{\beta}H$ Ser^{59}/$C^{\beta,\delta,\varepsilon}H$ Tyr^{64} and $C^{\beta}H$ Leu^{62}/$C^{\delta,\varepsilon}H$ Tyr^{64} protons.

(3) Search for the allowed side-chain conformations

χ^1 torsion angles of sB throughout the 20 best DIANA conformations are shown in Table 1. To refine the set of allowed side-chain rotamers we calculated penalty functions F_r and relative energies ΔE for all possible rotamers of each side chain in the α-helix involving C-terminal Tyr^{64}. To save CPU time, the energy was minimized and the function F_r was calculated within the $i \pm 5$ regions around each residue i. Initial values of χ_i^1 and χ_i^2 side-chain torsion angles were set according to the library of side-chain rotamers in proteins (Ponder and Richards, 1987) and χ_i^3, χ_i^4 were set to 180°, while other angles were the same as in the best DIANA conformation. In contrast to the distance geometry calculations, ambiguously assigned and overlapped cross peaks from protons in residues of the $i \pm 5$ region were regarded (see Eq. 9).

Figure 2 represents the penalty functions F_r and relative energies ΔE corresponding to side-chain rotamers around the C^{α}-C^{β} bond. A large F_r function (> 0.5 Å) means that there are several violated NOESY cross-peak volumes. For example, 7 cross peaks from 22 regarded possessed a distance mismatch Δr (Eq. 7) greater than 0.5 Å in the g^+ and g^- rotamers of Leu^{61} (cor-

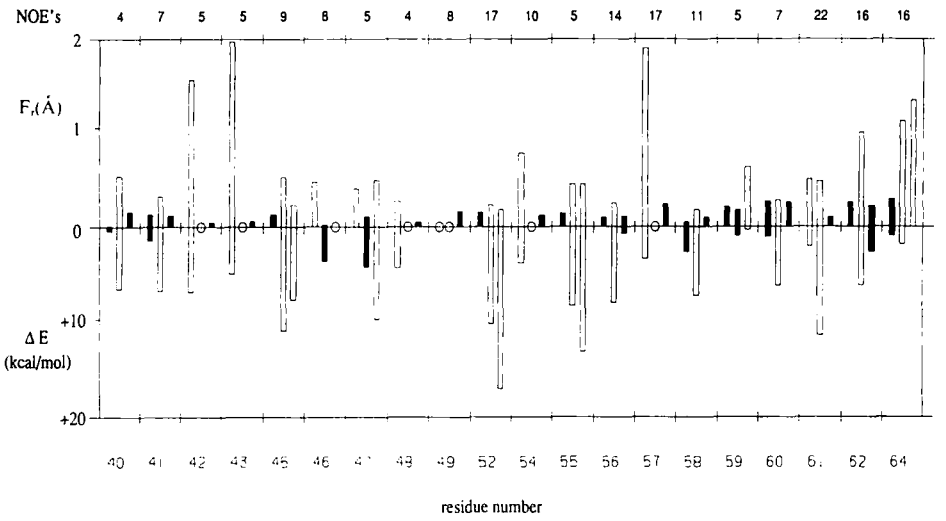

Fig. 2. Relative energies ΔE (kcal/mol) and F_r (Å) penalty functions (Eq. 6) calculated for the $i \pm 5$ region with g$^+$, g$^-$ and t rotamers of the C^α-C^β bond of residue i represented as 3 bars per residue. For each residue the first bar corresponds to the g$^+$ rotamer (with $\chi^1 \approx -60^\circ$), the second to the g$^-$ rotamer ($\chi^1 \approx 60^\circ$) and the last one to the t rotamer ($\chi^1 \approx 180^\circ$). The open circles indicate sterically unfavorable rotamers ($\Delta E > 20$ kcal/mol) usually disturbing the α-helix. The bars of allowed side-chain rotamers are filled. Amounts of NOESY cross peaks used for calculation of the F_r penalty function are shown in the upper panel. Cross peaks, which volumes weakly depend on the side-chain orientation, were excluded to get a better discrimination of side-chain rotamers.

responding F_r functions were 0.51 and 0.42 Å), while Δr was less than 0.15 Å for all cross peaks in the t rotamer of Leu^{61} with an F_r about 0.1 Å. All rotamers with an F_r less than 0.2 Å were considered to fit well to the NOESY data. Thus, the only rotamer was preferred for 11 residues on the basis of NOE data (Table 1).

When several rotamers met NOE data, we used the conformational energy as an additional criterion. So the rotamers with a relative energy (without electrostatic term) worse than 5 kcal/mol were discarded. The allowed side-chain rotamers for Ile^{45}, Ile^{52}, Nle^{56} and Nle^{60} residues were identified (Fig. 2).

(4) Random generation and energy refinement of sB conformations with allowed side-chain rotamers

To visualize the accessible conformational space of sB, we generated 20 conformations of sB with randomly selected allowed side-chain rotamers from the set obtained at step 3. These conformations were subjected to energy minimization with ECEPP/2 force fields and F_r and F_v penalty functions were calculated (Table 2). A superposition of these 20 conformations is shown in Fig. 3. The α-helical region 41–62 is well-defined since the pairwise atomic RMSD of 20 conformations is 0.38 Å for the backbone atoms (Table 2). The obtained conformations are energetically very close, since the ECEPP/2 energies are within -214 ± 3 kcal/mol.

The final set of sB conformations is well-consistent with NMR data. The F_r penalty function (RMS of interproton distance mismatches Δr for NOESY cross-peak volumes, see Eqs. 6–9) is only 0.33 Å. The individual Δr's are usually less than 0.5 Å, only few of them reached 1.0 Å (Table 2).

TABLE 2
ANALYSIS OF 20 ENERGY-REFINED CONFORMATIONS OF sB IN SDS MICELLES

Quantity[a]	Mean value ± standard deviation
Penalty function F_v	0.38 ± 0.01
Penalty function F_r (Å)	0.33 ± 0.01
Used NOE cross peaks	358
Number of NOE violations:	
with $\Delta r > 0.5$ Å	47 ± 3
with $\Delta r > 1.0$ Å	2 ± 1
Energy (kcal/mol)	−214 ± 3
Pairwise RMSD (Å) within residues 41–62	
of backbone atoms	0.38 ± 0.17
of all heavy atoms	0.83 ± 0.21

[a] Penalty functions F_r and F_v were calculated according to Eqs. 4 and 6. The Δr is the individual interproton distance mismatch characterized deviation of experimental and theoretical NOESY cross-peak volumes (Eq. 7).

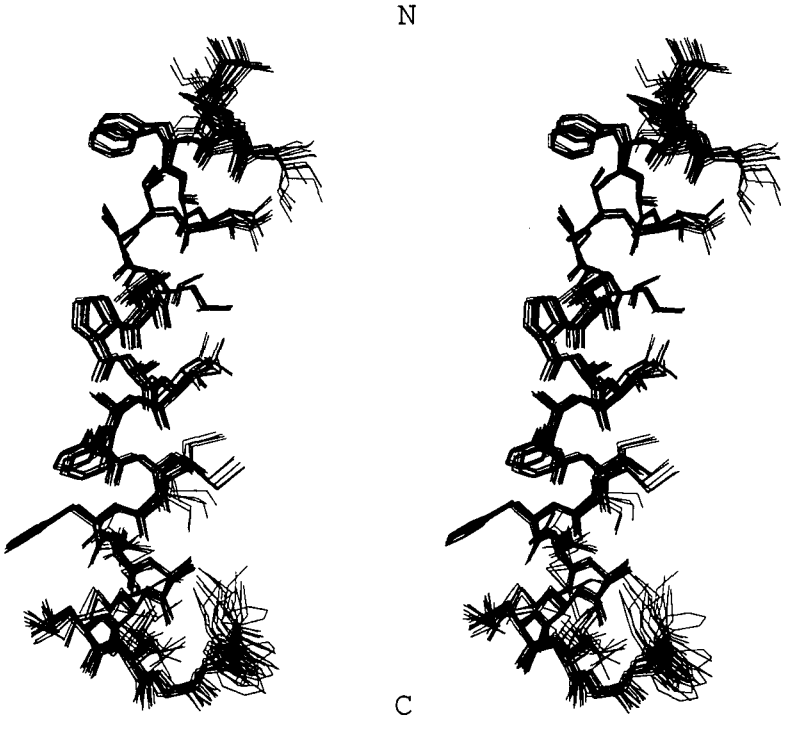

Fig. 3. Stereoview of the 20 energy-refined conformations of sB with randomly generated allowed side-chain rotamers. All heavy atoms are shown. Conformations were superimposed for a minimum RMSD of the backbone N, C^{α}, C' and O atoms of the Lys^{41}–Leu^{62} region.

χ^1 torsion angles were unequivocally determined for 13 of the 20 amino acid residues in the 39–64 region (Table 1) on the basis of combined use of NOE data and energy calculations, while χ^2 angles of Nle, Lys, Leu and Ile residues remain uncertain due to the lack of appropriate NMR data. The set of χ^1 angles is identical to that obtained by the program DIANA for 45% of the residues (see Table 1). Conformations of other side chains were refined by a search procedure. In few cases (Lys^{40}, Nle^{56}, Leu^{58} and Nle^{60}) two χ^1 rotamers of a side chain agree with experimental NOESY cross-peak volumes, but only one of them occurs among the DIANA conformations. This must be related to underestimation of upper interproton distance constraints $\{d_k\}$ used in DIANA calculations.

In other cases (see Tyr^{43}, Thr^{46}, Thr^{47} and Phe^{54} in Fig. 2) the DIANA output contains two different χ^1 side-chain rotamers, but only one of them fits well to NOESY cross-peak volumes. These side-chain conformations were refined as we used additionally 119 overlapped cross peaks, which were neglected in the DIANA calculations.

Comparison of sB structures in different environments

Figure 4 outlines the secondary structure of (34–65)bacterioopsin in SDS micelles and in methanol–chloroform mixture (Maslennikov et al., 1991b), as well as part of the BR chymotryptic C2 (residues 1–71) fragment in methanol–chloroform mixture (Sobol et al., 1992) and in the ECM BR model (Henderson et al., 1991). A rigid α-helical region of sB in SDS micelles is localized to residues 41–62. The α-helix is terminated by C-cap Gly^{63} in the left-handed helix conformation that leads to formation of the Tyr^{64} N-H...O = C Ser^{59} hydrogen bond. This is a common structural motif for α-helix termination (Schellman et al., 1980). The nonpolar part 42–65 of sB is appar-

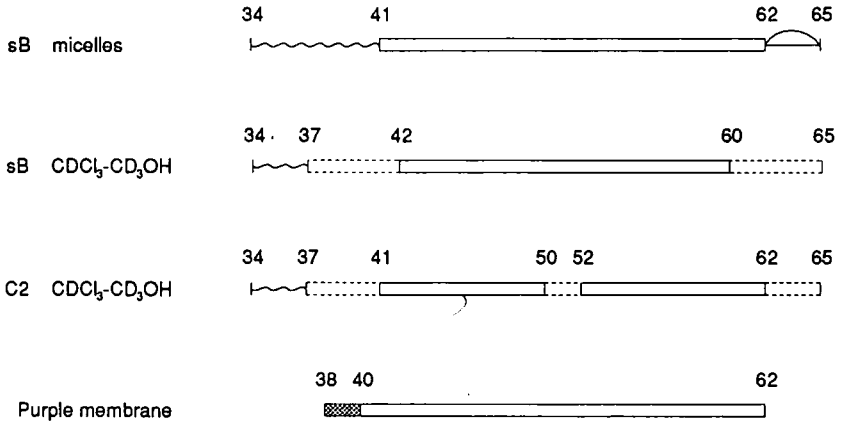

Fig. 4. Secondary structure of transmembrane segment B (sB) identified by ^1H NMR in SDS micelles, in chloroform–methanol (Maslennikov et al., 1991b), in the proteolytic C2 (residues 1–71) fragment of BR in chloroform–methanol (Sobol et al., 1992) and derived from the ECM model of BR (purple membrane) (Henderson et al., 1990). Solid rectangles denote the stable part of the α-helix with slow deuterium exchange of amide protons. Dashed rectangles indicate α-helical regions with fast deuterium exchange. Wave lines indicate disordered regions of polypeptide chain. The grey bar indicates residues from the ECM model that have no clear electron density at the experimental map but are assigned to the α-helix (Henderson et al., 1990).

ently incorporated into the micelle core, and the N-terminal hydrophilic region 34–41 is exposed to the aqueous phase and lacks an ordered conformation.

The α-helical region of sB in methanol–chloroform mixture is longer (residues 37–65) than that in SDS micelles, but the stable part of the α-helix includes only the 42–60 region. The side-chain conformations of sB in methanol–chloroform mixture and in SDS micelles are identical except Phe^{42}, Thr^{46}, Thr^{47} and Leu^{61} residues. These residues have two allowed side-chain rotamers in methanol–chloroform, but only one in SDS micelles. The chymotryptic C2 fragment of bacterioopsin in methanol–chloroform mixture appeared to have an α-helix identical to that of sB in the same milieu. The stable part of the α-helix of the C2 fragment is 3 residues longer than that of sB in methanol–chloroform and identical to that found in SDS micelles except two residues followed by Pro^{50} in the central part of the α-helix.

The characteristic feature of sB (Fig. 3) is a kink of the α-helix caused by Pro^{50}. The kink angle of 27° (between the axis of the 41–49 and 51–62 regions of the α-helix) is almost identical for all final sB conformations. This kink angle is characteristic to globular proteins containing a proline residue within their α-helices (Barlow and Thornton, 1988) and differs from the kink angle of 9° in the ECM BR model. The NH group of Ala^{51} forms a hydrogen bond with the CO group of Leu^{48} that is typical for the 3_{10} helix.

According to the ECM data, BR of purple membrane contains an α-helix located within the 38–62 region (Fig. 4), though Asp^{38} and Ala^{39} residues have no clear electron density on the experimental map (Henderson et al., 1991). Thus, the sB and C2 backbone conformations in artificial systems are in good agreement with the ECM model of the native BR structure.

The NMR study might play a unique role in the refinement of BR spatial structure and delineating conformations of BR fragments in artificial milieus. These conformations might be considered as building blocks of the entire molecule.

REFERENCES

Abdulaeva, G.V., Sobol, A.G., Arseniev, A.S., Tsetlin, V.I. and Bystrov, V.F. (1991) *Biol. Membrany (USSR)*, **8**, 30–34.

Arseniev, A.S., Kuryatov, A.B., Tsetlin, V.I., Bystrov, V.F., Ivanov, V.T. and Ovchinnikov, Yu.A. (1987) *FEBS Lett.*, **213**, 283–288.

Arseniev, A.S., Maslennikov, I.V., Kozhich, A.T., Bystrov, V.F., Ivanov, V.T. and Ovchinnikov, Yu.A. (1988) *FEBS Lett.*, **231**, 81–88.

Barlow, D.J. and Thornton, J.M. (1988) *J. Mol. Biol.*, **201**, 601–619.

Barsukov, I.L., Abdulaeva, G.V., Arseniev, A.S. and Bystrov, V.F. (1990) *Eur. J. Biochem.*, **192**, 321–327.

Bayley, H., Huang, K.S., Radhakrishnan, R., Ross, A.H., Takagaki, Y. and Khorana, H.G. (1981) *Proc. Natl. Acad. Sci. USA*, **78**, 2225–2229.

Bodenhausen, G. and Ernst, R.R. (1982) *J. Am. Chem. Soc.*, **104**, 1304–1309.

Bremer, J., Mendz, G.L. and Moore, W.J. (1984) *J. Am. Chem. Soc.*, **106**, 4691–4696.

Dencher, N.A. (1983) *Photochem. Photobiol.*, **38**, 753–767.

Güntert, P., Braun, W. and Wüthrich, K. (1991) *J. Mol. Biol.*, **217**, 517–530.

Henderson, R., Baldwin, J.M., Ceska, T.A., Zemlin, F., Beckmann, E. and Downing, K.H. (1990) *J. Mol. Biol.*, **213**, 899–929.

Keepers, J.W. and James, T.L. (1984) *J. Magn. Reson.*, **57**, 404–426.

Lomize, A.L., Sobol, A.G. and Arseniev, A.S. (1990) *Bioorgan. Chem. (USSR)*, **16**, 179–201.

Maslennikov, I.V., Arseniev, A.S., Kozhich, A.T., Bystrov, V.F. and Ivanov, V.T. (1990) *Biol. Membrany (USSR)*, **8**, 222–229.

Maslennikov, I.V., Arseniev, A.S., Chikin, L.D., Kozhich, A.T., Bystrov, V.F. and Ivanov, V.T. (1991a) *Biol. Membrany (USSR)*, **8**, 156–160.
Maslennikov, I.V., Lomize, A.L. and Arseniev, A.S. (1991b) *Bioorgan. Chem. (USSR)*, **17**, 1456–1469.
Momany, F.A., McGuire, R.F., Burgess, A.W. and Scheraga, H.A. (1975) *J. Phys. Chem.*, **79**, 2361–2381.
Nemethy, G., Pottle, M.S. and Scheraga, H.A. (1983) *J. Phys. Chem.*, **87**, 1883–1887.
Ovchinnikov, Yu.A. (1982) *FEBS Lett.*, **148**, 179–191.
Pervushin, K.V., Arseniev, A.S., Kozhich, A.T. and Ivanov, V.T. (1991) *J. Biomol. NMR*, **1**, 313–322.
Ponder, J.W. and Richards, F.M. (1987) *J. Mol. Biol.*, **193**, 775–791.
Schellman, C. (1980) In *Protein Folding* (Ed, Jaenick, R.) Elsevier, Amsterdam, pp. 53–61.
Sobol, A.G. and Arseniev, A.S. (1988) *Bioorgan. Chem. (USSR)*, **14**, 997–1013.
Sobol, A.G., Arseniev, A.S., Abdulaeva, G.V., Musina, L.Yu. and Bystrov, V.F. (1992) *J. Biomol. NMR*, **2**, 161–171.
Stoeckenius, W. (1985) *Trends Biochem. Sci.*, **10**, 483–486.
Tropp, J. (1980) *J. Chem. Phys.*, **72**, 6035–6043.